MOLECULAR AND CELLULAR BIOLOGY, June 1994, p. 3884–3894
0270-7306/94/$04.00+0

Vol. 14, No. 6

Tissue-Specific Expression of the Human CD19 Gene in Transgenic Mice Inhibits Antigen-Independent B-Lymphocyte Development

LIANG-JI ZHOU,[1,2] HEIDI M. SMITH,[1] THOMAS J. WALDSCHMIDT,[3] ROLAND SCHWARTING,[4] JOHN DALEY,[1] AND THOMAS F. TEDDER[1,2]*

Division of Tumor Immunology, Dana-Farber Cancer Institute, and Department of Pathology, Harvard Medical School, Boston, Massachusetts 02115-6084[1]; Department of Immunology, Duke University Medical Center, Durham, North Carolina 27710[2]; Department of Pathology, University of Iowa, Iowa City, Iowa 52242[3]; and Department of Pathology, Thomas Jefferson Medical College, Philadelphia, Pennsylvania 19107[4]

Received 28 September 1993/Returned for modification 24 November 1993/Accepted 11 March 1994

CD19 is a B-cell-specific member of the immunoglobulin superfamily expressed from early pre-B-cell development until plasma cell differentiation. In vitro studies demonstrate that the CD19 signal transduction molecule can serve as a costimulatory molecule for activation through other B-lymphocyte cell surface molecules. However, much remains to be known regarding how CD19 functions in vivo and whether CD19 has different roles at particular stages of B-cell differentiation. Therefore, transgenic mice overexpressing the human CD19 (hCD19) gene were generated to determine whether this transgene would be expressed in a B-lineage-specific fashion and to dissect the in vivo role of CD19 in B-cell development and activation. Expression of the human transgene product was specifically restricted to all B-lineage cells and appeared early in development as occurs with hCD19. In addition, expression of hCD19 severely impaired the development of immature B cells in the bone marrow, with dramatically fewer B cells found in the spleen, peripheral circulation, and peritoneal cavity. The level of hCD19 expressed on the cell surface correlated directly with the severity of the defect in different transgenic lines. These results demonstrate that the hCD19 gene is expressed in a lineage-specific fashion in mice, indicating that the hCD19 gene may be useful for mediating B-lineage-specific expression of other transgene products. In addition, these results indicate an important role for the lineage-specific CD19 molecule during early B-cell development before antigen-dependent activation.

B lymphocytes develop from multipotential stem cells and mature into antibody-secreting plasma cells after passing through multiple differentiation stages (reviewed in references 11 and 39). Pre-B cells express cytoplasmic μ heavy-chain protein before developing into immature B cells that express surface immunoglobulin M (IgM). This highly regulated process of early B-cell development is stromal cell dependent and antigen independent and occurs primarily in the bone marrow. Immediately prior to leaving the bone marrow, B cells mature to acquire surface IgM and IgD expression and the ability to respond to antigen. B cells also express other surface molecules important for B-cell development, proliferation, and differentiation (reviewed in reference 8). CD19 is a lineage-specific 95,000-M_r glycoprotein expressed by early pre-B cells from about the time of Ig heavy-chain rearrangement until plasma cell differentiation (27, 28). CD19 has two extracellular Ig-like domains, a membrane-spanning domain and a highly charged ~240-amino-acid cytoplasmic tail that has been well conserved during recent mammalian evolution (45, 53). CD19 is also a component of a multimeric cell surface signal transduction complex expressed by mature B cells which includes CD21 (CR2, C3d/Epstein-Barr virus receptor), CD81 (TAPA-1), and Leu-13 (5, 25).

CD19-mediated signal transduction initiates a series of biological responses that are likely to be of central importance to B-cell signaling and/or growth regulation (4, 6, 34, 36) and the development of a humoral immune response (15). Cross-linking of CD19 with a monoclonal antibody (MAb) induces an increase in the intracellular calcium ion concentration ($[Ca^{2+}]_i$) of B cells and some B-cell lines (5, 34, 49) and induces tyrosine kinase activity (7, 18). CD19 and surface Ig are functionally linked, because MAb binding to CD19 inhibits the increase in $[Ca^{2+}]_i$ that follows mitogen stimulation and subsequent B-cell activation and proliferation (34). On the other hand, ligation of surface Ig also leads to inactivation of normal calcium mobilization by cross-linked CD19 (37), and comodulation studies indicate that CD19 can cocap with cell surface Ig (33). CD19 MAb binding may also provide a proliferative signal for early IgM-negative precursor B cells (49). Furthermore, the Lyn, Lck, and Fyn protein tyrosine kinases may associated with CD19 (48, 50), and the cytoplasmic domain of CD19 contains kinase insert regions that when phosphorylated mediate the binding and activation of phosphatidylinositol 3-kinase (47). Thus, although the precise in vivo function of CD19 has not been definitively elucidated, these studies support the hypothesis that the CD19 complex can serve an accessory role in conjunction with surface Ig to enhance antigen-driven B-cell activation (6).

Although CD19 is one of the first lineage-specific surface molecules expressed during early pre-B-cell development, little is known about the functional importance of this molecule during early B-cell differentiation or the role of CD19 in vivo. However, the expression of cloned genes in transgenic mice can provide a direct readout of biological consequences of receptor function rather than the effects evoked following cross-linking of a receptor with MAb as has primarily been the approach for examining CD19 function. Further, the mouse model allows an analysis of the complex signaling pathways that occur during early B-cell hematopoiesis for which satisfactory tissue culture models do not exist. Therefore, the human CD19 (hCD19) gene was microinjected into mouse

* Corresponding author. Present address: Department of Immunology, Duke University Medical Center, Box 3010, Durham, NC 27710. Phone: (919) 684-4119. Fax: (919) 684-8982.

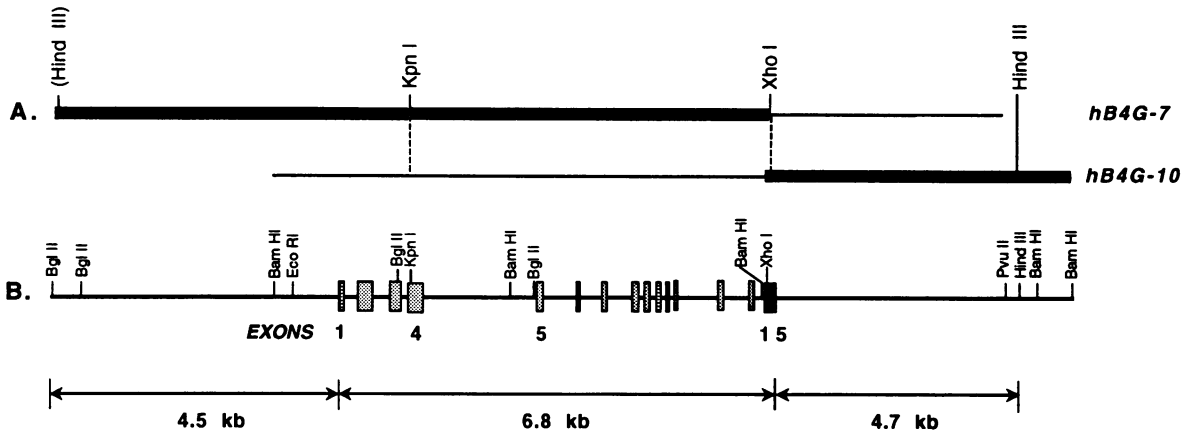

FIG. 1. Structure of the hCD19 transgene. (A) DNA fragments from human genomic DNA clones hB4G-7 (*Hin*dIII to *Kpn*I and *Kpn*I to *Xho*I) and hB4G-10 (*Xho*I to *Hin*dIII) were linearly assembled to produce the transgene. The *Hin*dIII site in hB4G-7 enclosed in parentheses was located in the polylinker of the DNA clone. (B) Intron-exon organization of the transgene containing exons 1 through 15 with 4.5 kb of 5′ flanking and 4.7 kb of 3′ flanking sequence. Exons are indicated by rectangles; speckled rectangles indicate translated sequence.

eggs to determine whether appropriate expression of this gene would occur in mice and to produce mice with augmented overall CD19 expression. Since MAb reagents are available only for hCD19, use of the hCD19 gene also allowed the direct analysis of transgene expression which could be assessed independently of endogenous mouse CD19 (mCD19). These studies revealed that expression of the hCD19 gene in mice was completely B cell restricted. In addition, examination of the effect of hCD19 expression on mouse B-cell function revealed that the hCD19 gene product severely altered normal B-cell development, demonstrating that CD19 is an important factor in regulating early B-cell generation and maturation.

MATERIALS AND METHODS

CD19 transgene construction. The hCD19 transgene was constructed in the SP65 plasmid by the sequential insertion of fragments of genomic DNA containing the CD19 gene and flanking sequences (Fig. 1). Two DNA fragments from the genomic clone hB4G-7 (52), from the 5′ end of the clone to the unique internal *Kpn*I site and from the *Kpn*I site to the *Xho*I site, were subcloned into a plasmid with the *Xho*I-*Hin*dIII fragment of the 3′ end of the gene from genomic clone hB4G-10. The total length of the transgene was ~16 kb, with ~4.5 kb of 5′ flanking sequence and ~4.7 kb of 3′ flanking sequence. Unique *Hin*dIII restriction sites flanked the transgene, allowing linearization and separation from the vector. Linearized transgene was first purified by electrophoresis on agarose gels followed by ion-exchange column chromatography using Qiagen columns (Qiagen, Inc., Chatsworth, Calif.) or Elutip-D columns (Schleicher & Schuell, Keene, N.H.). The purified linear hCD19 gene DNA was microinjected into the male pronucleus of fertilized mouse eggs obtained from B6SJL female mice mated to males of the same cross. The eggs were reimplanted into pseudopregnant mice as described previously (17). Transgenic founder mice were mated with C57BL/6J mice to propagate the transgenic lines. All progeny were identified as heterozygous or homozygous for the hCD19 gene by examining the gene copy number relative to the parental transgenic mice and human DNA.

Southern and Northern (RNA) blot analyses. Mouse genomic DNA was extracted from the distal 1 to 1.5 cm of tails from 3-week-old mice as described previously (17). Southern blot analysis was performed as described elsewhere (43, 46). Ten micrograms of restriction endonuclease-digested DNA was electrophoresed in horizontal 0.8% agarose gels and transferred to nitrocellulose (51). Human DNA was isolated from Epstein-Barr virus-transformed blood lymphocytes. hCD19 cDNA inserts were isolated from plasmids, twice purified by agarose gel electrophoresis, ^{32}P labeled by nick translation (35), and hybridized with the filters as described previously (43). Hybridization was performed at 42°C in the presence of 50% (vol/vol) formamide, and the filters were washed with 0.2× SSC (1× SSC is 0.15 M NaCl plus 0.015 M sodium citrate) with 0.1% (wt/vol) sodium dodecyl sulfate at 65°C. DNA fragment size was determined by coelectrophoresis of a 1-kb ladder (Bethesda Research Laboratories, Gaithersburg, Md.). The hCD19 cDNA probe, pB4-17, was similar to the published pB4-19 cDNA (45) except that it begins with the G of the translation initiation codon and terminates 22 nucleotides 3′ of the poly(A) attachment signal sequence and has 17 3′ A's attached. Three discontinuous mCD19 cDNAs, mB4-211A1, mB4-30, mB4-503.1, that span from nucleotide position 98 to the poly(A) tail as shown previously (53) were used as probes for Southern analysis.

RNA was extracted from tissues dissociated with a homogenizer (Konet Glass Co., Vineland, N.J.) in the presence of 4 M guanidine isothiocyanate as described previously (42). Northern blot analysis was carried out with formaldehyde as a denaturing reagent. Ten micrograms of total cellular RNA was run in each lane, and intact RNA was visualized in the agarose gel by using ethidium bromide. pB4-17 was used as the probe, with hybridization at 42°C in the presence of 50% formamide. The nitrocellulose filter was washed in 0.2× SSC at 65°C after hybridization. mRNA size was determined by comparison with 28S and 18S rRNAs.

Determination of transgene copy number. Transgene copy number was determined by quantifying the level of hybridization of a hCD19 cDNA (AP17-1) probe with the same amount of genomic DNA from the human Namalwa B-cell line, normal mice, and transgenic mice blotted onto nitrocellulose. The counts per minute obtained for triplicate dot blot determinations was compared with the counts per minute obtained with human DNA which contains two copies of the CD19 gene.

Antibodies and serum Ig determinations. The following MAbs were used in the flow cytometry analysis: phycoerythrin

(PE)-conjugated B4 (anti-hCD19; Coulter Corp., Hialeah, Fla.) and M1/69 (anti-mouse heat-stable antigen; Pharmingen, San Diego, Calif.); fluorescein isothiocyanate (FITC)-conjugated RA3-6B2 (anti-CD45R/B220) (9), B4 (anti-hCD19; Coulter), 145-2C11 (anti-mCD3) (22), HO13.4 (anti-Thy1.2) (24), Ig(5a)7.2 (anti-mouse IgDa allotype) (30), Ig(5b)6.3 (anti-mouse IgDb allotype) (31), S7 (anti-mCD43) (9), and 53-7.8 (anti-Ly-1; Pharmingen); and biotin-conjugated M1/70 (anti-Mac-1) (40), 6C3 (anti-BP-1; Pharmingen), S7, and RA3-6B2. Cyanine 5.18-conjugated RA3-6B2 and Texas red-conjugated goat anti-mouse IgM (Southern Biotechnology Associates, Birmingham, Ala.) were used in three- or four-color staining experiments. Polyclonal antisera, FITC-conjugated goat anti-mouse IgM (Southern Biotechnology Associates), and biotinylated goat anti-mouse IgM (Vector Laboratories, Burlingame, Calif.) were also used. Unconjugated HB12b (anti-hCD19) (5) and goat anti-mouse IgM (Southern Biotechnology Associates) were used in calcium flux experiments.

Ig levels in sera were determined by using an enzyme-linked immunosorbent assay (ELISA). Briefly, ELISA plates (Costar, Cambridge, Mass.) were coated with 100 μl (10 μg/ml) of goat anti-mouse IgG1, IgG2a, IgM, and IgA antibodies (Southern Biotechnology Associates) at 4°C overnight. After three washes with phosphate-buffered saline (PBS) containing 0.1% bovine serum albumin (BSA), the plates were blocked by PBS with 1% fetal calf serum and 0.02% sodium azide for 1 h at 37°C. The plates were washed three times, and diluted mouse serum was incubated at 37°C for 2 h. Affinity-purified mouse Igs of all isotypes (Southern Biotechnology Associates) were used as standards in the assay. Plates were washed four times with PBS–0.1% BSA and further incubated with alkaline phosphatase-conjugated isotype-specific goat anti-mouse Ig (2 μg/ml; Southern Biotechnology Associates) for 2 h at 37°C. Finally, alkaline phosphatase substrate *p*-nitrophenyl phosphate (Sigma, St. Louis, Mo.) was added to the plates at 1 mg/ml to visualize positive reactions. Optical density values were collected by using a spectrophotometer (Titertek Multiskan MC; Flow Laboratories, McLean, Va.) at a 405-nm wavelength.

Cells and immunofluorescence analysis. Single-cell suspensions of mouse peripheral blood leukocytes, splenocytes, thymocytes, bone marrow cells, and peritoneal cavity cells were isolated and examined immediately by immunofluorescence analysis. One-color direct immunofluorescence analysis was performed as described previously (9) by using FITC-conjugated B220 (RA3-6B2) and an anti-B4 MAb. Two-color immunofluorescence staining was performed by using FITC-conjugated antibodies in combination with biotinylated antibodies. Streptavidin-PE (Fisher Scientific, Fair Lawn, N.J.) was used to reveal biotin-coupled antibody staining. Cells were washed and analyzed on an EPICS Profile flow cytometer (Coulter). Ten thousand cells were analyzed for each sample. For three- and four-color staining, cells were incubated with FITC-, cyanine-, Texas red-, and biotin-conjugated antibodies for 20 min on ice, washed, and incubated with PE-avidin (Vector Laboratories). Anti-FcγR II antibody (2.4G2; 25 μg) and normal rat serum (10%, final volume) were added in the first step to eliminate nonspecific staining. Cells were analyzed on a modified dual-laser Becton Dickinson FACS 440 flow cytometer (Becton Dickinson Immunocytometry Systems, San Jose, Calif.), with a minimum of 30,000 cells collected per sample. The data were processed on a VAXstation 3200 computer equipped with FACS/DESK software (kindly supplied by Wayne Moore, Stanford University, Stanford, Calif.).

Cell cycle analysis. Single-cell suspensions of bone marrow cells were stained with B220-FITC and biotinylated anti-IgM antibody. Streptavidin-PE was used to visualize IgM staining. After being fixed with 4% formaldehyde (Fisher Scientific), the cells were incubated with the DNA dye DAPI (4′,6-diamidino-2-phenylindole; 5 μM; Molecular Probes, Eugene, Oreg.) in 0.4 M sodium phosphate buffer for 5 min on ice and then analyzed on a EPICS Elite flow cytometer (Coulter) as described previously (32). The DNA content of $B220^{dull}$ IgM^- (pro- and pre-B cells) and $B220^+$ IgM^+ (immature and mature B cells) was quantified, and the variability of DNA content was then analyzed mathematically.

Tissues and immunohistochemistry. Normal tissues were obtained from transgenic mice and their littermates and kept in liquid nitrogen until use. Frozen tissue sections were air dried overnight and subsequently fixed in acetone for 10 min. The sections were incubated with a biotinylated primary anti-CD19 MAb (HB12) for 30 min, washed with Tris-buffered saline (pH 7.8), and processed as described previously (12).

Measurement of $[Ca^{2+}]_i$. Mouse spleen cells were isolated as a single-cell suspension, treated with anti-CD3 and anti-Thy-1.2 MAbs, and incubated with baby rabbit serum (Pel-Freeze, Brown Deer, Wis.) to lyse T cells. Spleen B cells (10×10^6 to 30×10^6) in 1 to 2 ml of RPMI 1640 medium were loaded with 1 μM indo-1-acetoxymethyl (indo-1-AM) ester (Molecular Probes) at 37°C for 30 min, washed, and then resuspended at 0.5×10^6 cells per ml in RPMI 1640. For analysis, the ratio of fluorescence (525/405 nm) of cells (5×10^5 cells in 1-ml samples) was determined in an EPICS Elite flow cytometer. Baseline fluorescence ratios were collected for 30 s before specific MAbs were added. The CD19 MAb was added at a 1/200 final dilution of ascites fluid, and goat anti-mouse IgM antiserum (Southern Biotechnology Associates) was added at a 1/500 final dilution of the antiserum supplied by the manufacturer. A decrease in the fluorescence ratio indicates an increase in $[Ca^{2+}]_i$.

Statistics. All statistical comparisons were carried out by using the one- or two-tailed Student's *t* test.

RESULTS

Production of hCD19 transgenic mice. To determine whether the regulatory elements necessary for lineage-specific expression of CD19 were proximal to known exons (52), a transgene including all hCD19 exons, 4.5 kb of 5′ upstream DNA, and 4.7 kb of 3′ DNA (Fig. 1) was injected into mouse eggs. Eight of thirty-seven mice, termed h19-1 through h19-8, carried the hCD19 gene, and seven of the founder lines expressed hCD19 on the cell surface at high (hCD19-1) to low (hCD19-7) levels (Table 1). Although the founder mice were chimeric for the transgene, 40 to 80% of the $B220^+$ B cells were $hCD19^+$ (Table 1; Fig. 2). Four of the founder mice generated offspring with germ line transmission frequencies of 67, 10, 67, and 25% for the h19-1, -4, -5, and -7 lines, respectively. Transgene copy number varied from ~1 to ~14 in the different lines, with a positive correlation between gene dosage and the intensity of hCD19 expression (Table 1; Fig. 2). In homozygous transgenic mice, cell surface hCD19 expression was ~2-fold higher than that of the heterozygous mice, and all $hCD19^+$ cells expressed B220 (Fig. 2). Thus, the regulatory elements necessary to mediate hCD19 expression in murine cells were present in the transgene.

Expression of the hCD19 transgene is limited to B cells. Northern blot analysis of RNA isolated from various organs of heterozygous h19-1 mice and control littermates revealed hCD19 expression only in the spleens of transgenic mice (Fig. 3). The predominant mRNA species was ~2.4 kb, with additional species of 2.8, 3.1, and 3.7 kb, as seen in human B cells

TABLE 1. Characteristics of blood lymphocytes from hCD19 transgenic mice

Line	Gene copy no.	% Positive cells[a]						
		Founder mice			Heterozygous mice		Homozygous mice	
		Sex[b]	CD19$^+$	B220$^+$	CD19$^+$	B220$^+$	CD19$^+$	B220$^+$
Control	0	M + F	0	60 ± 13	0	60 ± 12	0	60 ± 12
h19-1	9–14	M	13 ± 3	26 ± 5[c]	23 ± 2	23 ± 6[d]	7 ± 2	7 ± 2[d]
h19-2	ND[e]	F	11 ± 7	25 ± 9[f]				
h19-3	1–2	F	12 ± 1	40 ± 4				
h19-4	2–3	M	12 ± 4	53 ± 15	46 ± 1	46 ± 1	30 ± 3	30 ± 3[d]
h19-5	1–2	F	17 ± 14	30 ± 13[f]	41 ± 2	41 ± 1[f]	30 ± 2	30 ± 2[c]
h19-6	ND	F	7 ± 3	37 ± 15				
h19-7	1–2	M	3 ± 2	52 ± 2	45 ± 1	45 ± 1	49 ± 1	49 ± 1
h19-8	ND	M	1 ± 1	61 ± 7				

[a] Values represent percentages of positive cells for a given surface antigen obtained from blood lymphocytes (based on side-angle and forward light scatter) and represent results obtained on at least three different occasions for the founder mice and results from at least three heterozygous and homozygous mice. In all instances, the background percentages of cells that were positive (<3%) were subtracted from the values presented. The frequency of fluorescence-positive cells was determined by single-color analysis using a Coulter Profile flow cytometer.

[b] M, male; F, female.

[c] Significantly less than in control littermates ($P < 0.01$).

[d] Significantly less than in control littermates ($P < 0.002$).

[e] ND, not determined.

[f] Significantly less than in control littermates ($P < 0.05$).

(45). When the same Northern blot was probed with an mCD19 cDNA probe under high-stringency conditions, only RNA from the spleens of transgenic and control mice hybridized (data not shown). The levels of hybridization were identical between transgenic and control mice, indicating that expression of the hCD19 gene had no obvious effect on endogenous mCD19 expression.

Cells from bone marrow, spleens, thymuses, peripheral blood, and peritoneal cavities of transgenic mice were examined for hCD19 expression by immunofluorescence staining. Only B220$^+$ cells from these tissues expressed the hCD19 transgene (Fig. 2 and 4). In all cell populations examined, CD3$^+$ or Thy1.2$^+$ T cells, monocytes, granulocytes, or other hematopoietic cells failed to express hCD19. Similar results were obtained for all founder mice and for their heterozygous and homozygous offspring. Among bone marrow cells, all surface IgM$^+$ cells were hCD19$^+$ (Fig. 4). However, consistent with the very early appearance of B220 in B-cell development, not all B220$^+$ cells were hCD19$^+$. Nonetheless, a substantial proportion of hCD19$^+$ cells were pro- or pre-B cells, since only 50% of hCD19$^+$ cells expressed surface IgM. Furthermore, ~10% of hCD19$^+$ cells expressed CD43 (S7), which identified early pro-B cells, and 20% of the hCD19$^+$ cells expressed the BP-1/6C3 marker present on late pro-B or pre-B cells (Fig. 5). Also, it was very obvious that hCD19 expression increased while pro-B cells matured from S7$^+$ B220$^+$ to BP-1$^+$ B220$^+$ to B220$^+$ IgM$^+$ B cells (Fig. 5). Therefore, hCD19 transgene expression was restricted to the B lineage, and the transgene was expressed during early pro- and pre-B-cell development as occurs in humans.

Immunohistochemical staining of mouse spleen, lymph node, thymus, brain, heart, kidney, liver, lung, stomach, small intestine, uterus, and skin tissue sections of transgenic mice revealed that expression of hCD19 was restricted to B-lineage cells (Fig. 6). Expression of hCD19 was not detected in normal mouse tissues. hCD19$^+$ cells were found in the B-cell areas of lymph nodes and in the white pulp and red pulp of spleens in both heterozygous and homozygous h19-1 animals. It was not possible to determine whether follicular dendritic cells within germinal centers expressed CD19 as occurs in humans (41). Some hCD19$^+$ lymphocytes were found in the small intestine and the thymus medulla, consistent with the rare presence of B cells in these tissues.

B-cell development is impaired in hCD19 transgenic mice. Expression of the hCD19 transgene correlated inversely with the number of circulating B220$^+$ cells: high levels of hCD19 expression resulted in decreased numbers of circulating B cells (Fig. 2; Table 1). This effect was particularly apparent in homozygous and heterozygous transgenic mice (Table 1). Heterozygous h19-1 mice had only 22% of control numbers of circulating B cells ($P < 0.001$), while homozygous mice had only 4% of normal numbers ($P < 0.001$) (Fig. 7). Similarly, spleen weight in 2- to 3-month-old homozygous transgenic mice was reduced by 30 to 40%, and the h19-1 transgenic mice had only 65% as many spleen B cells ($P = 0.016$), while homozygous mice had only 18% of the normal number ($P < 0.001$). In contrast, the numbers of circulating and spleen T cells in the transgenic mice were not significantly different from those in control mice (Fig. 7).

B-cell development in hCD19 transgenic mice was significantly impaired. Most noticeable was that the B220^{bright} IgM$^+$ (Fig. 4A) or IgM$^+$ IgD$^+$ (data not shown) mature B-cell population in bone marrow was either significantly reduced or absent ($P < 0.001$) compared with the level in control littermates. On average, the frequency of B220^{bright} IgM$^+$ cells was reduced by 54% in 2- to 3-month-old heterozygous mice and by 73% in homozygous animals (Fig. 8). The h19-1 transgenic mice also had significantly fewer newly generated B220^{dull} IgM$^+$ B cells in the bone marrow, with a 35% reduction ($P = 0.007$) in heterozygous mice and 64% reduction ($P < 0.001$) in homozygous mice. However, the percentage of IgM$^-$ B220$^+$ cells was not apparently changed in 2-month-old mice, suggesting no accumulation of pre-B cells in the bone marrow despite the decrease in B-cell frequency. Consistent with this finding, the frequencies of CD43$^+$ B220$^+$ cells were similar in control (3.6% ± 2.0%, $n = 3$) and homozygous (5.2% ± 2.5%, $n = 5$) littermates (Fig. 5). Also, the frequencies of BP-1/6C3-positive cells were 4.0% ± 2.8% ($n = 5$) in homozygous transgenic mice and 5.4% ± 0.6% ($n = 3$) in control littermates (Fig. 5). Thus, early pro-B- and pre-B-cell development was not significantly impaired, while the generation of immature B cells

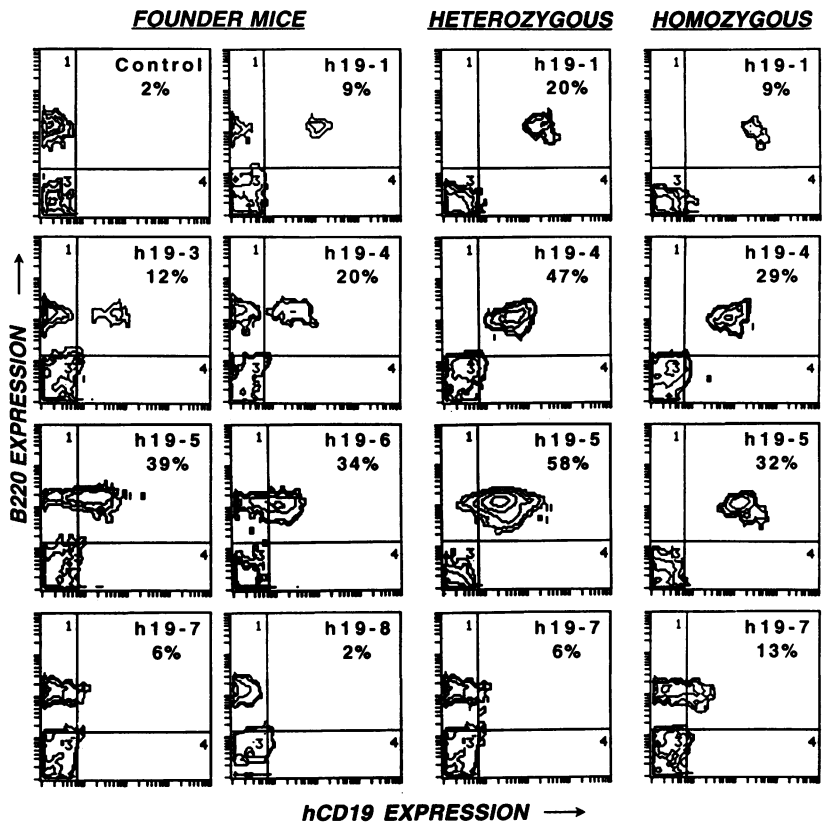

FIG. 2. hCD19 expression by blood leukocytes from control and transgenic mice. All studies were carried out at the same time by two-color analysis using the CD19 MAb (B4) conjugated to PE and the B220 MAb labeled with FITC. Fluorescence analysis was on a Coulter Elite flow cytometer. Founder mice were 14 months old and the heterozygous and homozygous progeny were 2 months old at the time of analysis. Values for each histogram represent the percentages of $CD19^+$ $B220^+$ cells in the total lymphocyte population gated on forward and side-angle light scatter. Horizontal and vertical lines which divide the figures into four quadrants delineate negative and positive populations of cells as determined by using an unreactive control MAb. Fluorescence intensity is shown on a four-decade log scale. These values differ from results obtained for single-color analysis (Table 1) because of the requirement for compensation during two-color analysis, which lowers the fluorescence intensity of hCD19 staining.

($B220^{dull}$ IgM^+) and mature B cells ($B220^{bright}$ IgM^+) was dramatically reduced.

Similar results were obtained with 2-week-old h19-1 transgenic mice (Fig. 4B) except that the proportion of IgM^+ B-lineage cells in the bone marrow was more sharply reduced: 66% in heterozygous mice and 88% in homozygous mice. The frequency of $B220^+$ cells was also lower: 52% reduced in heterozygous mice and 69% reduced in homozygous mice. However, the frequency of IgM^- $B220^+$ cells was not dramatically reduced between control (20%, $n = 2$), heterozygous (16%, $n = 2$), or homozygous (14%, $n = 2$) littermates. The frequency of B cells in the spleen of 2-week-old transgenic mice was also significantly decreased. In the 19-1 line, control littermates had 23×10^6 ($\pm 3 \times 10^6$, $n = 2$) splenic B cells, compared with 17×10^6 ($\pm 5 \times 10^6$, $n = 2$) for heterozygous mice and 2×10^6 ($\pm 1 \times 10^6$, $n = 2$) for homozygous mice. These results indicate that the bone marrow of transgenic mice might produce normal numbers of IgM^- $B220^+$ pre-B cells and that the apparent block in B-cell development induced by hCD19 expression occurred during the late stages of pre-B-cell development or at the time of surface IgM expression.

The frequency of bone marrow pre-B and B cells in the cell cycle was determined in 2-month-old littermates to determine whether the defect in B-cell development resulted from an arrest of cell proliferation. In two experiments, the frequencies

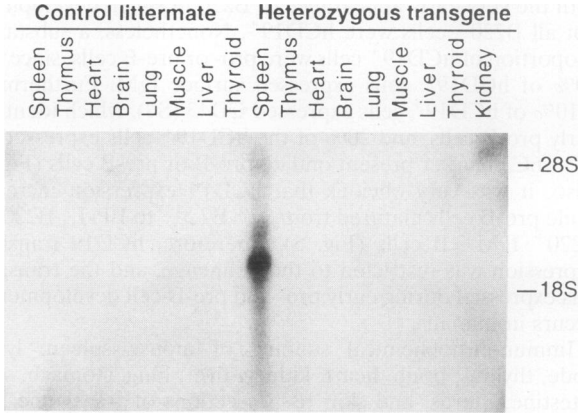

FIG. 3. The hCD19 transgene is expressed in the spleens of transgenic mice but not in other tissues. A Northern blot of RNA from tissues of a heterozygous h19-1 mouse and a control littermate was probed with labeled pB4-17 hCD19 cDNA. Nitrocellulose filters were washed under high-stringency conditions so that the hCD19 cDNA does not bind to mCD19 mRNA. rRNA was run in parallel as an indicator of size and to verify that the RNA was intact. Autoradiography was for 1 week with an intensifying screen.

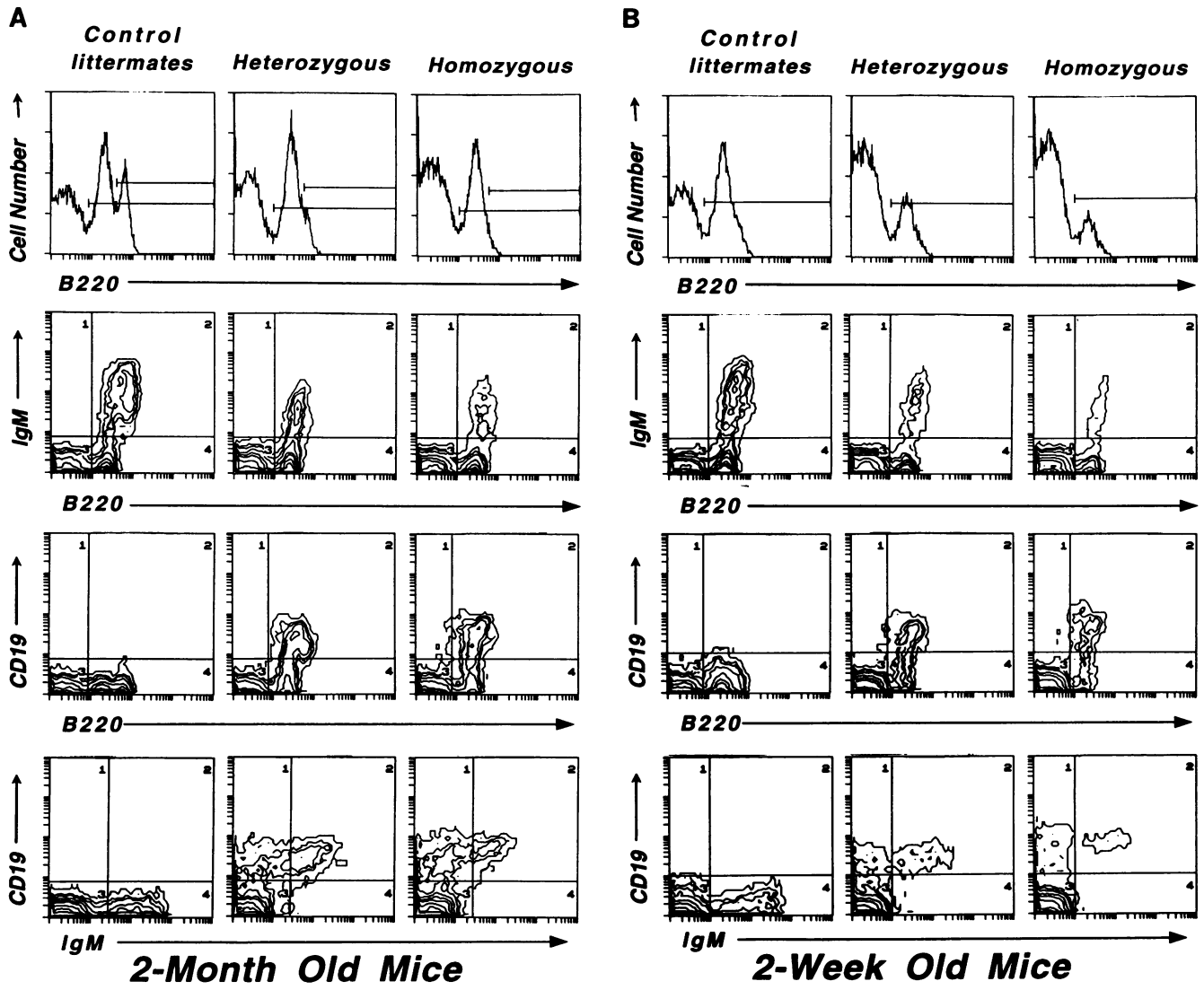

FIG. 4. Expression of hCD19 by bone marrow cells from h19-1 mice. (A) Results are representative of those obtained from 2-month-old control (−/−; n = 7), heterozygous (+/−; n = 4), or homozygous (+/+; n = 6) littermates. (B) Results are representative of those obtained from 2-week-old control (−/−; n = 2), heterozygous (+/−; n = 2), or homozygous (+/+; n = 2) littermates. Data are presented as in Fig. 2.

of IgM^- $B220^+$ pre-B cells in G_1, S, and G_2/M were 80 to 85, 15 to 20, and <1%, respectively, in control mice and 75 to 86, 14 to 25, and <1%, respectively, in homozygous h19-1 mice. In the IgM^+ $B220^+$ B-cell compartment, the frequencies of cells in G_1, S, and G_2/M were 96 to 98, 0 to 1.4, and 0.5 to 4.2%, respectively, in control mice and 95 to 99, 0 to 5.3, and 0 to 0.4%, respectively, in homozygous h19-1 mice. Therefore, cell cycle progression was not appreciably affected by hCD19 expression.

Although unlikely, one explanation for the decrease in peripheral B-cell numbers in the hCD19 transgenic mice could be the production of antibodies or cytotoxic T cells reactive with hCD19, leading to removal of the B cells through immune-effector mechanisms. However, antibody specific for hCD19 was not detected in serum from five homozygous h19-1 mice (data not shown). Further, since hCD19 would be an endogenous protein in the transgenic mice, there is no reason to suspect that cytotoxic T cells should be generated against this molecule, and there was no evidence of abnormal T-cell infiltrates into tissues in which hCD19 was expressed (Fig. 6).

Signal transduction through hCD19. Spleen B cells isolated from homozygous h19-1 mice increased $[Ca^{2+}]_i$ in response to binding of the anti-human CD19 MAb alone (Fig. 9). Spleen cells from control and h19-1 mice also increased $[Ca^{2+}]_i$ to equivalent levels in response to optimal doses of anti-mouse Ig antibodies, demonstrating that the calcium signaling pathway in the transgenic mice was functional (Fig. 9). The addition of the anti-hCD19 MAb in combination with a suboptimal concentration of anti-mouse Ig antibody also resulted in an increase in the percentage of h19-1 spleen cells which increased $[Ca^{2+}]_i$ (data not shown). The addition of the anti-hCD19 MAb alone or with suboptimal amounts of anti-mouse Ig antibodies to spleen cells from control littermates did not alter $[Ca^{2+}]_i$ levels, consistent with these cells not expressing hCD19 (Fig. 2). Thus, hCD19 expressed in mouse cells is capable of signal transduction.

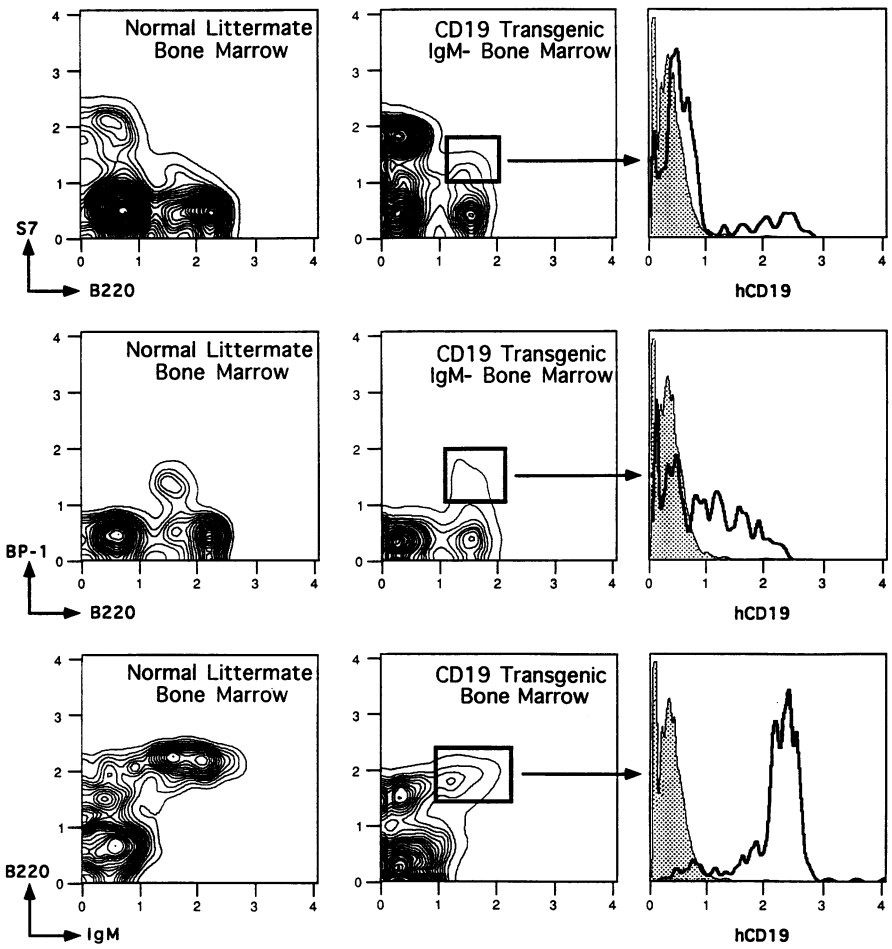

FIG. 5. B-cell development in homozygous hCD19 transgenic mice. Early pro-B- and pre-B-cell development is not significantly altered in the transgenic mice, whereas immature ($B220^{dull}$ IgM^+) and mature ($B220^{bright}$ IgM^+) B-cell numbers decreased dramatically, as revealed by two-, three-, and four-color fluorescence staining and flow cytometry analysis of bone marrow with antibodies to S7, BP-1, B220, and IgM. hCD19 expression increased as B cells matured from $S7^+$ $B220^+$ to $BP\text{-}1^+$ $B220^+$ to IgM^+ $B220^+$ stages.

The abilities of B cells to mature into Ig-producing plasma cells were compared in four 2- to 3-month-old homozygous h19-1 transgenic mice and control littermates. IgM (1.3 ± 0.4 mg/ml [control] versus 5.0 ± 5.0 mg/ml [transgenic]), IgG1 (1.6 ± 0.8 versus 3.1 ± 0.3), IgG2a (0.28 ± 0.08 versus 0.22 ± 0.8), and IgA (3.4 ± 1.7 versus 3.6 ± 1.5) levels were not significantly different. Therefore, the hCD19 transgenic mice were not notably immunocompromised.

DISCUSSION

The pattern of hCD19 gene expression in transgenic mice demonstrated that all necessary B-cell-specific regulatory elements were contained within the transgene (Fig. 1). Among blood and bone marrow leukocytes, only B lymphocytes expressed the transgene product (Fig. 2 and 4). In addition, hCD19 mRNA was found only in hematopoietic tissues (Fig. 3), and only the B-cell areas in spleen, lymph nodes, and other tissues contained hCD19 protein (Fig. 6). Regulation of hCD19 expression during B-cell development in transgenic mice was similar to that observed in humans, with expression starting at the early pro- and pre-B-cell stages of differentiation (Fig. 4 and 5) and continuing through B-cell maturation. Like CD19, the endogenous promoter and enhancer regions of the Ig light- and heavy-chain genes are active early in the lymphocyte lineage, but expression of the Ig heavy-chain promoter is not completely B cell restricted in transgenic mice (14, 21, 29). Therefore, the CD19 gene may be similar to the κ light-chain gene, which can initiate B-cell-specific expression of foreign gene products (44). Although the κ light-chain gene shares no significant homology with the CD19 gene, the CD19 gene contains sequences similar to the NFκB and μB motifs (52). Binding sites for the B-cell-specific activator protein/Pax-5 transcription regulatory factor have also been identified in the CD19 promoter region (2, 20), although B-cell-specific activator protein/Pax-5 is found in the central nervous system and testis (2, 3). In contrast to many other transgenes, there was a positive correlation between the number of hCD19 transgene copies and the surface expression of hCD19, with homozygous transgenic mice expressing ~2-fold-higher levels of hCD19 than heterozygous mice (Fig. 2). The CD19 regulatory elements thus provide a model of lineage-specific gene regulation and may also provide a promoter element useful for manipulation, since expression of the hCD19 gene was B cell specific and without obvious insertional effects.

Expression of hCD19 inhibited the early development of mouse B-lineage cells. The number of immature IgM^+

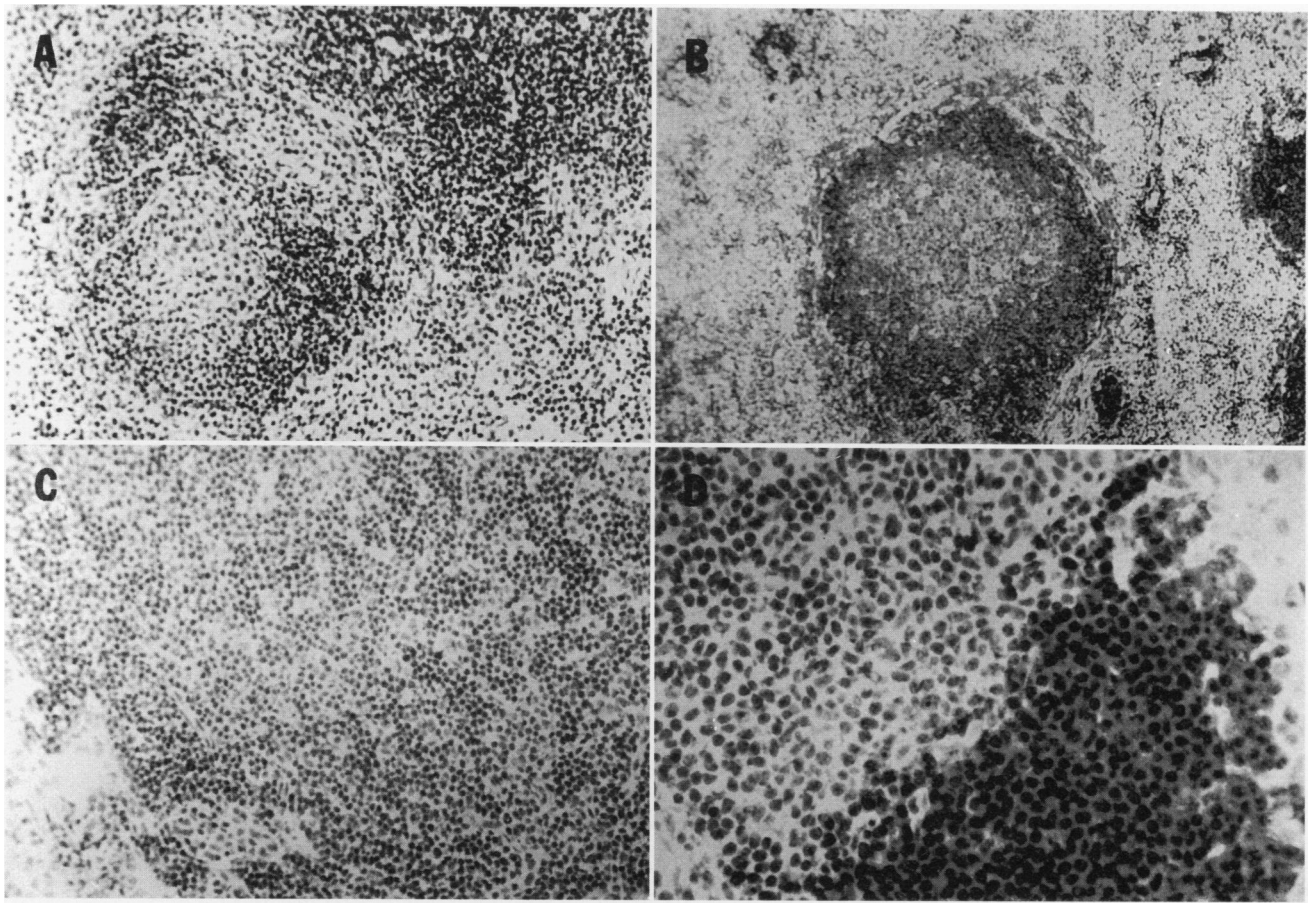

FIG. 6. Immunohistochemical analysis of hCD19 transgene expression in heterozygous transgenic hCD19-1 mice (B and D) and control littermates (A and C). Follicular B-cell areas in spleen (A and B [magnification, ×200]) and lymph node (C [magnification, ×200] and D [magnification, ×400]) were $hCD19^+$ in transgenic mice, while no cells in control mice were $hCD19^+$ as determined by the APAAP (mouse anti-alkaline phosphatase antibody previously reacted with alkaline phosphatase) staining technique.

$B220^{dull}$ B cells and mature $B220^{bright}$ IgM^+ IgD^+ B cells in the bone marrow of transgenic mice was significantly reduced (Fig. 4, 5, and 8). In contrast, the percentage of pro- and pre-B cells in the bone marrow did not change dramatically, indicating that early B-cell development was not significantly inhibited and that pro- and pre-B cells did not accumulate (Fig. 4, 5, and 8). Expression of hCD19 did not completely obstruct B-cell maturation, since B cells were found in blood, lymphoid organs, and the peritoneal cavity, but at significantly lower frequencies (Fig. 2 and 7). Although the presence of B cells presumably reflects the peripheral expansion of mature B lymphocytes, the accumulation of peripheral B cells did not compensate for the effect of the hCD19 transgene, since old mice had a comparable deficit in B-cell numbers (Fig. 2). Similar results were obtained in all transgenic lines, with the severity of the defect correlating with the level of hCD19 expression (Table 1; Fig. 2). This dose-response effect in independent lines of mice directly implicates hCD19 as the cause of impaired B-cell development rather than an indirect effect resulting from inappropriate insertion of the transgene into the genome.

Whereas impairment of B-cell development was correlated with the number of cell surface hCD19 molecules expressed (Fig. 5), this increase in receptor number may translate into the overproduction of a necessary signal which results in altered regulation of B-cell development. It is also possible

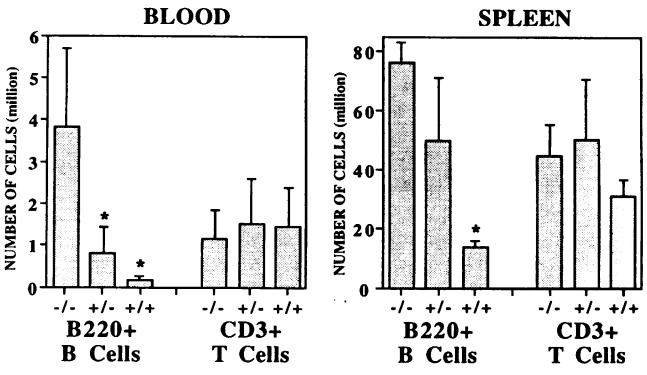

FIG. 7. hCD19 expression in transgenic mice alters the frequency of B lymphocytes in blood and spleen. The numbers of lymphocytes were based on the determined number of blood leukocytes per unit volume and the total number of mononuclear cells isolated from spleens of 2- to 3-month-old mice. The percentage of $B220^+$ B cells and $CD3^+$ T cells was then determined by flow cytometry. Results represent mean values (± standard deviations) obtained for blood isolated from 12 control, 10 heterozygous, and 9 homozygous littermates and with spleen cells isolated from 6 control, 6 heterozygous, and 4 homozygous littermates.

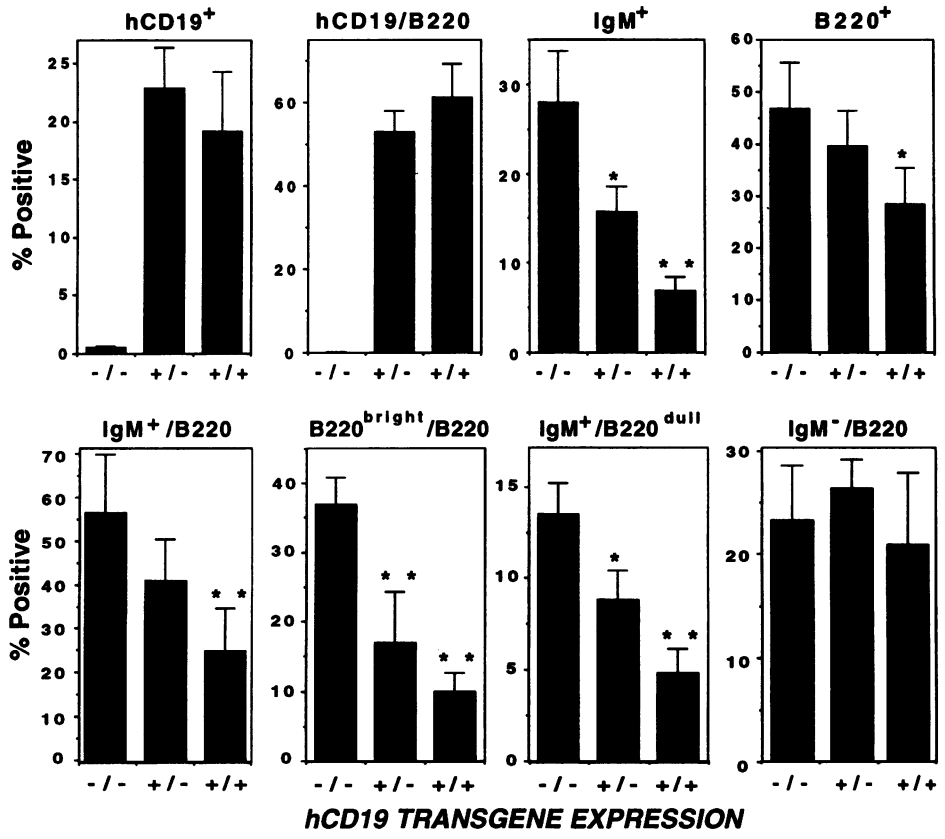

FIG. 8. Lymphocyte populations present in bone marrow of hCD19 transgenic mice. These data are a summary (means ± standard deviations) of results similar to those shown in Fig. 4 for 2-month-old h19-1 mice: control littermates (−/−; $n = 7$), heterozygous mice (+/−; $n = 4$), and homozygous mice (+/+; $n = 6$). Values represent percentages of lymphocytes expressing the indicated cell surface markers and were determined by two-color immunofluorescence staining with flow cytometry analysis. For example, hCD19/B220 represents the percentage of $B220^+$ cells that are $hCD19^+$. *, significant difference relative to control littermates ($P \leq 0.007$); **, $P \leq 0.001$.

that intracellular kinases or other members of the mCD19 complex bind the human molecule and are thereby not available for proper signal transduction through mCD19, since the amino acid sequence homology between mCD19 and hCD19 is high (45). The paucity of B cells in CD19 transgenic mice does not result from blocking B-cell activation, since B cells from transgenic and control littermates were equivalent in their early responses to IgM cross-linking (Fig. 9), and h19-1 transgenic mice had normal levels of serum Ig of all isotypes. Further, increased CD19 numbers did not result in desensitization of other signal transduction pathways, since cross-linking of hCD19 or IgM in the transgenic mice induced a potent change in $[Ca^{2+}]_i$ (Fig. 9). Increased turnover of pre-B and B cells in the bone marrow did not account for the differences in B-cell numbers, since cell cycle differences between transgenic and control littermates were not observed and the pre-B-cell population was normal in size. The hCD19-induced defect did not result from significant alterations in endogenous mCD19 mRNA levels, since they were not affected by expression of the hCD19 gene. These findings demonstrate that hCD19 is functional in mouse B cells and that the inhibition of early B-cell development may result from the generation of inappropriate signals rather than secondary effects resulting from expression of a nonfunctional hCD19 receptor. Thus, it is likely that the extracellular domain of hCD19 binds to a putative mCD19 receptor or generates the appropriate functional cell surface receptor complex and that the cytoplasmic portion of hCD19 interacts with mouse intracellular signaling molecules.

The phenotype of the hCD19 transgenic mice is similar to that of mice expressing μ or δ heavy-chain transgenes which have a decrease in the total pool of peripheral B cells (13, 16, 26). This is presumed to result from the premature expression of a heavy-chain product resulting in a shorter transit time in the bone marrow maturation pathway and eventually resulting in the decreased expansion of the B-cell pool. The phenotype of the hCD19 transgenic mice is more likely to reflect a disruption of normal mCD19 function, thereby providing a toxic or suppressive signal during early B-cell development. Similarly, doubling the steady-state level of $p56^{lck}$ in transgenic mice impairs thymocyte development (1). Overexpression of CD8 in T cells impairs thymus development as a result of increased negative selection of thymocytes (38). It is therefore possible that CD19 plays a similar role in the selection of B cells during early development. Expression of the hCD19 transgene also mimics the effects of dominant negative mutations which disrupt normal signal transduction in other experimental situations. In this respect, expression of a catalytically inactive $p56^{lck}$ transgene blocks early T-cell development in the thymus (23), while expression of a catalytically inactive version of $p59^{fyn}$ disrupts T-cell receptor-induced signaling without affecting thymocyte development (10). Interestingly however, the phenotype of the hCD19 transgenic mice was similar to that of mice in which the λ5 gene is inactivated by targeted

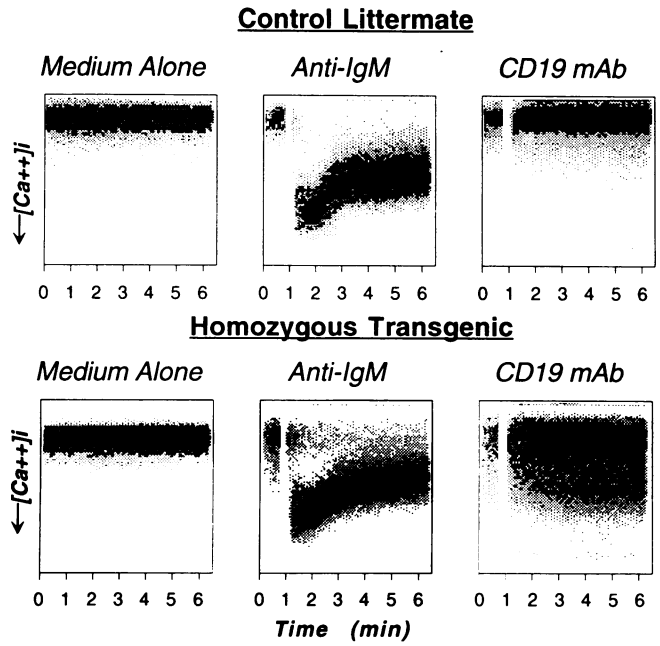

FIG. 9. Signal transduction through hCD19 in homozygous h19-1 spleen B cells. B cells were isolated from the spleens of homozygous h19-1 mice or control littermates. These cells were then loaded with indo-1 and treated with the anti-hCD19 (HB-12b) MAb, an optimal amount of anti-mouse IgM antibody, or medium alone. An increase in $[Ca^{2+}]_i$ over time is shown as a decrease in the ratio of indo-1 fluorescence. The gap in the histogram represents the time point at which the MAb was added.

disruption (9). Nonetheless, the results from this study suggest an important biological role for CD19 in the regulation of B-cell development in vivo and implicate CD19 in the regulation of both the incidence and rate of B-cell generation.

Since the defect in B-lymphocyte development occurred initially in the bone marrow microenvironment, a site of antigen-independent B-cell development (39), CD19 may function in regulating antigen-independent B-cell activation or survival during the late pre-B-cell stage or the period of transition from a pre-B cell into an immature B cell. While it is also likely that the CD19 complex is involved in B-cell function at later stages of maturation, understanding the functional role of the diverse groups of cell surface signal transduction molecules expressed early in B-cell development will provide a clear insight into the molecular mechanisms which direct B-cell differentiation. Also, several members of the CD19 cell surface complex are expressed by nonhematopoietic tissues, suggesting that similar regulatory processes may occur in other tissues involving receptors similar to CD19.

ACKNOWLEDGMENTS

We thank R. Noelle for serum Ig determinations and D. Ord, L. Bradbury, N. Wagner, P. Engel, and D. Weaver for helpful comments.

This work was supported by NIH grants CA-26872, AI-26872, and CA-34183 to T.F.T. and by NIH grant AI-31265. T.F.T. is a Scholar of the Leukemia Society of America.

REFERENCES

1. **Abraham, K. M., S. D. Levin, J. D. Marth, K. A. Forbush, and R. M. Perlmutter.** 1991. Delayed thymocyte development induced by augmented expression of $p56^{lck}$. J. Exp. Med. **173:**1421–1432.
2. **Adams, B., P. Dorfler, A. Aguzzi, Z. Kozmik, P. Urbanek, I. Maurer-Fogy, and M. Busslinger.** 1992. Pax-5 encodes the transcription factor BSAP and is expressed in B lymphocytes, the developing CNS, and adult testis. Genes Dev. **6:**1589–1607.
3. **Barberis, A., K. Widenhorn, L. Vitelli, and M. Busslinger.** 1990. A novel B-cell lineage-specific transcription factor present at early but not late stages of differentiation. Genes Dev. **4:**849–859.
4. **Barrett, T. B., G. L. Shu, K. E. Draves, A. Pezzutto, and E. A. Clark.** 1990. Signaling through CD19, Fc receptors or transforming growth factor-β: each inhibits the activation of resting human B cells differently. Eur. J. Immunol. **20:**1053–1059.
5. **Bradbury, L., G. S. Kansas, S. Levy, R. L. Evans, and T. F. Tedder.** 1992. CD19 is a component of a signal transducing complex on the surface of B cells that includes CD21, TAPA-1 and Leu-13. J. Immunol. **149:**2841–2850.
6. **Carter, R. H., and D. T. Fearon.** 1992. CD19: lowering the threshold for antigen receptor stimulation of B lymphocytes. Science **256:**105–107.
7. **Carter, R. H., D. A. Tuveson, D. J. Park, S. G. Rhee, and D. T. Fearon.** 1991. The CD19 complex of B lymphocytes. Activation of phospholipase C by a protein tyrosine kinase-dependent pathway that can be enhanced by the membrane IgM complex. J. Immunol. **147:**3663–3671.
8. **Clark, E. A., and J. A. Ledbetter.** 1989. Structure, function, and genetics of human B cell-associated surface molecules. Adv. Cancer Res. **52:**81–149.
9. **Coffman, R. L., and I. L. Weissman.** 1981. B220: a B cell specific member of the T200 glycoprotein family. Nature (London) **289:** 681–685.
10. **Cooke, M. P., K. M. Abramah, K. A. Forbush, and R. M. Perlmutter.** 1991. Regulation of T cell receptor signalling by a src family protein-tyrosin kinase ($p59^{fyn}$). Cell **65:**281–291.
11. **Cooper, M. D.** 1987. B lymphocytes. Normal development and function. N. Engl. J. Med. **317:**1452–1456.
12. **Cordell, J., B. Fllini, O. N. Erber, A. K. Ghosh, Z. Abdulaziz, S. MacDonald, K. Polford, H. Stein, and D. Y. Mason.** 1984. Immunoenzymatic labelling of monoclonal antibodies using immune complexes of alkaline phosphatase and monoclonal anti-alkaline phosphatase (APAAP complexes). J. Histochem. Cytochem. **31:** 219–229.
13. **Era, T., M. Ogawa, S.-I. Nishikawa, M. Okamoto, T. Honjo, K. Akagi, J.-I. Miyazaki, and K.-I. Yamamura.** 1991. Differentiation of growth signal requirement by B lymphocyte precursor is directed by expression of immunoglobulin. EMBO J. **10:**337–342.
14. **Grosschedl, R., D. Weaver, D. Baltimore, and F. Costantini.** 1984. Introduction of a μ immunoglobulin gene into the mouse germ line: specific expression in lymphoid cells and synthesis of functional antibody. Cell **38:**647–658.
15. **Hebell, T., J. M. Ahearn, and D. T. Fearon.** 1991. Suppression of the immune response by a soluble complement receptor of B lymphocytes. Science **254:**102–105.
16. **Herzenberg, L. A., A. M. Stall, J. Braun, D. Weaver, D. Baltimore, L. A. Herzenberg, and R. Grosschedl.** 1987. Depletion of the predominant B-cell population in immunoglobulin μ heavy-chain transgenic mice. Nature (London) **329:**71–73.
17. **Hogan, B., F. Costantini, and E. Lacy.** 1986. Manipulating the mouse embryo: a laboratory manual. Cold Spring Harbor Laboratory, Cold Spring Harbor, N.Y.
18. **Kansas, G. S., and T. F. Tedder.** 1991. Transmembrane signals generated through MHC class II, CD19, CD20, CD39, and CD40 antigens induce LFA-1-dependent and independent adhesion in human B cells through a tyrosine kinase-dependent pathway. J. Immunol. **147:**4094–4102.
19. **Kitamura, D., A. Kudo, S. Schall, W. Muller, F. Melchers, and K. Rajewsky.** 1992. A critical role of λ5 protein in B cell development. Cell **69:**823–831.
20. **Kozmik, Z., S. Wang, P. Dorfler, B. Adams, and M. Busslinger.** 1992. The promoter of the CD19 gene is a target for the B-cell-specific transcription factor BSAP. Mol. Cell. Biol. **12:**2662–2672.
21. **Lamers, M. C., M. Vakil, J. F. Kearney, J. Langhorne, C. J. Paige, M. H. Julius, H. Mossmann, R. Carsetti, and G. Kohler.** 1989. Immune status of a u, k transgenic mouse line. Deficient response to bacterially related antigens. Eur. J. Immunol. **19:**459–468.

22. **Leo, O., M. Foo, D. H. Sachs, and L. E. Samalson.** 1987. Identification of a monoclonal antibody specific for a murine T3 polypeptide. Proc. Natl. Acad. Sci. USA **84:**1374–1378.
23. **Levin, S. D., S. J. Anderson, K. A. Forbush, and R. M. Perlmutter.** 1993. A dominant-negative transgene defines a role for $p56^{lck}$ in thymopoiesis. EMBO J. **12:**1671–1680.
24. **Marshak-Rothstein, A., P. Fink, T. Gridley, D. H. Raulet, M. J. Bevan, and M. L. Gefter.** 1979. Properties and applications of monoclonal antibodies directed against determinants of the THY-1 locus. J. Immunol. **122:**2491–2497.
25. **Matsumoto, A. K., J. Kopicky-Burd, R. H. Carter, D. A. Tuveson, T. F. Tedder, and D. T. Fearon.** 1991. Intersection of the complement and immune systems: a signal transduction complex of the B lymphocyte containing complement receptor type 2 and CD19. J. Exp. Med. **173:**55–64.
26. **Muller, W., U. Ruther, P. Vieira, J. Hombach, M. Reth, and K. Rajewsky.** 1989. Membrane-bound IgM obstructs B cell development in transgenic mice. Eur. J. Immunol. **19:**923–928.
27. **Nadler, L. M., K. C. Anderson, G. Marti, M. Bates, E. Park, J. F. Daley, and S. F. Schlossman.** 1983. B4, a human B lymphocyte-associated antigen expressed on normal, mitogen activated, and malignant B lymphocytes. J. Immunol. **131:**244–250.
28. **Nadler, L. M., S. J. Korsmeyer, K. C. Anderson, A. W. Boyd, B. Slaughenhoupt, E. Park, J. Jensen, F. Coral, R. J. Mayer, S. E. Sallan, J. Ritz, and S. F. Schlossman.** 1984. B cell origin of non-T cell acute lymphoblastic leukemia. A model for discrete stages of neoplastic and normal pre-B cell differentiation. J. Clin. Invest. **74:**332–340.
29. **Nussenzweig, M. C., A. C. Shaw, E. Sinn, D. B. Danner, K. L. Holmes, H. C. Morse III, and P. Leder.** 1987. Allelic exclusion in transgenic mice that express the membrane form of immunoglobulin μ. Science **236:**816–819.
30. **Oi, V. T., and L. A. Herzenberg.** 1979. Localization of murine Ig-1b and Ig-1a (IgG2a) allotypic determinants detected by monoclonal antibodies. Mol. Immunol. **16:**1005–1017.
31. **Oi, V. T., P. P. Jones, J. W. Gording, and L. A. Herzenberg.** 1978. Properties of monoclonal antibody to mouse Ig allotypes, H-2, and Ia antigens. Curr. Top. Microbiol. Immunol. **81:**115–129.
32. **Otto, F.** 1990. DAPI staining of fixed cells for high-resolution flow cytometry of nuclear DNA. Methods Cell Biol. **33:**105–110.
33. **Pesando, J. M., L. S. Bouchard, and B. E. McMaster.** 1989. CD19 is functionally and physically associated with surface immunoglobulin. J. Exp. Med. **170:**2159–2164.
34. **Pezzutto, A., B. Dorken, P. S. Rabinovitch, J. A. Ledbetter, G. Moldenhauer, and E. A. Clark.** 1987. CD19 monoclonal antibody HD37 inhibits anti-immunoglobulin-induced B cell activation and proliferation. J. Immunol. **138:**2793–2799.
35. **Rigby, P. W., M. Dieckmann, C. Rhodes, and P. Berg.** 1977. Labeling DNA to high specific activity *in vitro* by nick translation. J. Mol. Biol. **113:**237–251.
36. **Rigley, K. P., and R. E. Callard.** 1991. Inhibition of B cell proliferation with CD19 monoclonal antibodies: CD19 antibodies do not interfere with early signalling events triggered by anti-IgM or IL-4. Eur. J. Immunol. **21:**535–540.
37. **Rijkers, G. T., A. W. Griffioen, B. J. M. Zegers, and J. C. Cambier.** 1990. Ligation of membrane immunoglobulin leads to inactivation of the signal-transducing ability of membrane immunoglobulin, CD19, CD21, and B-cell gp95. Proc. Natl. Acad. Sci. USA **87:**8766–8770.
38. **Robey, E. A., F. Ramsdell, D. Kioussis, W. Sha, D. Loh, R. Axel, and B. J. Fowlkes.** 1992. The level of CD8 expression can determine the outcome of thymic selection. Cell **69:**1089–1096.
39. **Rolink, A., and F. Melchers.** 1991. Molecular and cellular origins of B lymphocyte diversity. Cell **66:**1081–1094.
40. **Sanchez-Madrid, F., P. Simon, S. Thompson, and T. A. Springer.** 1983. Mapping of antigenic and functional epitopes on the α- and β-subunit of two related mouse glycoproteins involved in cell interactions, LFA-1 and Mac-1. J. Exp. Med. **158:**586–602.
41. **Schriever, F., A. S. Freedman, G. Freeman, E. Messner, G. Lee, J. Daley, and L. M. Nadler.** 1989. Isolated human follicular dendritic cells display a unique antigenic phenotype. J. Exp. Med. **169:**2043–2058.
42. **Sleasman, J. W., C. Morimoto, S. F. Schlossman, and T. F. Tedder.** 1990. The role of functionally distinct helper T lymphocyte subpopulations in the induction of human B cell differentiation. Eur. J. Immunol. **20:**1357–1366.
43. **Southern, E. M.** 1975. Detection of specific sequence among DNA fragments separated by gel electrophoresis. J. Mol. Biol. **98:**503–517.
44. **Storb, U., R. L. O'Brien, M. D. McMullen, K. A. Gollahon, and R. L. Brinster.** 1984. High expression of cloned immunoglobulin κ gene in transgenic mice is restricted to B lymphocytes. Nature (London) **310:**238–241.
45. **Tedder, T. F., and C. M. Isaacs.** 1989. Isolation of cDNAs encoding the CD19 antigen of human and mouse B lymphocytes: a new member of the immunoglobulin superfamily. J. Immunol. **143:**712–717.
46. **Tedder, T. F., G. Klejman, S. F. Schlossman, and H. Saito.** 1989. Structure of the gene encoding the human B lymphocyte differentiation antigen CD20 (B1). J. Immunol. **142:**2560–2568.
47. **Tuveson, D. A., R. H. Carter, S. P. Soltoff, and D. T. Fearon.** 1993. CD19 of B cells as a surrogate kinase insert region to bind phosphatidylinositol 3-kinase. Science **260:**986–989.
48. **Uckun, F. M., A. L. Burkhardt, L. Jarvis, X. Jun, B. Stealey, I. Dibirdik, D. E. Myers, L. Tuel-Ahlgren, and J. B. Bolen.** Signal transduction through the CD19 receptor during discrete developmental stages of human B-cell ontogeny. J. Biol. Chem., in press.
49. **Uckun, F. M., and J. A. Ledbetter.** 1988. Immunobiologic differences between normal and leukemic human B-cell precursors. Proc. Natl. Acad. Sci. USA **85:**8603–8607.
50. **van Noesel, C. J. M., A. C. Lankester, and R. A. W. van Lier.** 1993. Dual antigen recognition by B cells. Immunol. Today **14:**8–11.
51. **Wahl, G. M., M. Stern, and G. R. Stark.** 1979. Efficient transfer of large DNA fragments from agarose gels. Proc. Natl. Acad. Sci. USA **76:**3683–3687.
52. **Zhou, L.-J., D. C. Ord, S. A. Omori, and T. F. Tedder.** 1992. Structure of the genes encoding the CD19 antigen of human and mouse B cells. Immunogenetics **35:**102–111.
53. **Zhou, L.-J., D. C. Ord, A. L. Hughes, and T. F. Tedder.** 1991. Structure and domain organization of the CD19 antigen of human, mouse and guinea pig B lymphocytes. Conservation of the extensive cytoplasmic domain. J. Immunol. **147:**1424–1432.